



Isocitrate dehydrogenase1 mutation reduces the pericyte coverage of microvessels in astrocytic tumours

Chao Sun^{1,2} · Yuanlin Zhao² · Jiankuan Shi^{2,3} · Jin Zhang² · Yuan Yuan² · Yu Gu² · Feng Zhang² · Xing Gao² · Chao Wang⁴ · Yingmei Wang² · Zhe Wang² · Peizhen Hu² · Junhui Qin² · Liming Xiao² · Ting Chang¹ · Liang Wang⁵ · Yibin Xi⁶ · Hong Yin⁶ · Huangtao Chen⁷ · Lijun Zhang⁸ · Guang Cheng⁹ · Jiaji Lin¹ · MingMing Zhang¹⁰ · Zhuyi Li¹ · Jing Ye^{1,2}

Received: 12 January 2019 / Accepted: 21 March 2019
© Springer Science+Business Media, LLC, part of Springer Nature 2019

Abstract

Introduction Tumour-associated angiogenesis is associated with the malignancy and poor prognosis of glioma. Isocitrate dehydrogenase (IDH) mutations are present in the majority of lower-grade (WHO grade II and III) and secondary glioblastomas, but their roles in tumour angiogenesis remain unclear.

Methods Using magnetic resonance imaging (MRI), the cerebral blood flow (CBF) of IDH-mutated glioma was measured and compared with the IDH-wildtype glioma. The densities of microvessels in IDH-mutated and wildtype astrocytoma and glioblastoma were assessed by immunohistochemical (IHC) staining with CD34, and the pericytes were labelled with α -smooth muscle antigen (α -SMA), neural-glial antigen 2 (NG2) and PDGF receptor- β (PDGFR- β), respectively. Furthermore, glia-specific mutant IDH1 knock-in mice were generated to evaluate the roles of mutant IDH1 on brain vascular architectures. The transcriptions of the angiogenesis-related genes were assessed in TCGA datasets, including ANGPT1, PDGFB and VEGFA. The expressions of these genes were further determined by western blot in U87-MG cells expressing a mutant IDH1 or treated with 2-HG.

Results The MRI results indicated that CBF was reduced in the IDH-mutated gliomas. The IHC staining showed that the pericyte coverages of microvessels were significantly decreased, but the microvessel densities (MVDs) were only slightly decreased in IDH-mutated glioma. The mutant IDH1 knock-in also impeded the pericyte coverage of brain microvessels in mice. Moreover, the TCGA database showed the mRNA levels of angiogenesis factors, including ANGPT1, PDGFB and VEGFA, were downregulated, and their promoters were also highly hyper-methylated in IDH-mutated gliomas. In addition, both mutant IDH1 and D-2-HG could downregulate the expression of these genes in U87-MG cells.

Conclusions Our results suggested that IDH mutations could reduce the pericyte coverage of microvessels in astrocytic tumours by inhibiting the expression of angiogenesis factors. As vascular pericytes play an essential role in maintaining functional blood vessels to support tumour growth, our findings imply a potential avenue of therapeutic strategy for IDH-mutated gliomas.

Keywords Glioma · Angiogenesis · Isocitrate dehydrogenase · Pericytes

Electronic supplementary material The online version of this article (<https://doi.org/10.1007/s11060-019-03156-5>) contains supplementary material, which is available to authorized users.

Chao Sun, Yuanlin Zhao, and Jiankuan Shi contributed equally as first authors.

✉ Zhuyi Li
lizhuyi@fmmu.edu.cn

✉ Jing Ye
yejing@fmmu.edu.cn

Extended author information available on the last page of the article

Introduction

Gliomas are highly vascularized brain tumours, and vascular abnormality correlates with the malignancy grades of glioma and poor prognoses in glioma patients [1]. Although anti-angiogenic therapy shows some effective clinical benefits in gliomas, the survival of glioma patients has not been improved substantially. Consistent with the normal vasculature, tumour vessels consist of two distinct but interdependent cellular compartments, namely, endothelial cells (ECs)

and pericytes [2]. Vascular pericytes play critical roles in supporting vascular structure and function, facilitating initiating vessel sprouting and vessel maturation [2, 3]. Vascular pericytes contribute to support vessel function [4], and the increased coverage of vascular pericytes is the main constituent of microvessels (MVs) in high-grade gliomas [5], which might protect ECs and render ECs less responsive to anti-angiogenic agents [4]. Recent studies have focused on the roles and morphological features of glioma vascular pericytes, but there is no data whether glioma genotype alters vascular pericytes.

Genomic analysis reveals mutations in the active sites of isocitrate dehydrogenases (IDH) in 70–80% of lower-grade gliomas (LGGs) and secondary glioblastomas (GBM) [6]. Oncogenic IDH mutations gain a new activity to catalyse the NADPH-dependent reduction of α -ketoglutarate (α -KG) to D-2-hydroxyglutarate (D-2-HG). As an oncometabolite [6–8], D-2-HG competitively inhibits α -KG-dependent dioxygenases, including histone demethylases and the ten-eleven translocation (TET) family of 5-methylcytosine hydroxylases, resulting in complex genetic and epigenetic alterations [9]. Recently, it was reported that a mutant IDH1 knock-in resulted in severe brain haemorrhage in mice [10], and IDH mutations affected the tumour blood flow in gliomas [11, 12], which implies that IDH mutations contribute to the abnormality and dysfunction of glioma vasculature. The clinical data have indicated that IDH-mutant glioma patients have a better prognosis than those with wildtype IDH, but the functions of IDH mutations in the angiogenesis and vascular architecture of glioma remains unclear.

In this study, the cerebral blood flow (CBF) and vascular architecture of microvessels were investigated in IDH-mutated and IDH-wildtype astrocytic tumours (astrocytomas and glioblastomas), to explore the roles of IDH mutations on the structural and functional aspects of glioma vasculature.

Materials and methods

Glioma samples

All glioma tissue slides were collected from the Department of Pathology at Xijing Hospital of Fourth Military Medical University, including 29 astrocytoma (Grade II), 21 anaplasia astrocytoma (Grade III) and 34 GBM (Grade IV) samples. Fresh glioma specimens were obtained from the Department of Neurosurgery at Tangdu Hospital of Fourth Military Medical University. The pathological diagnoses of these glioma samples were confirmed by experienced neuropathologists according to the 2016 WHO criteria for classification of CNS tumours. The IDH status was determined by Sanger sequencing, and the 1p/19q co-deletion was analysed using fluorescent in situ hybridization (FISH) assays.

Arterial spin labelling

Arterial spin labelling (ASL) was acquired using pseudo-continuous labelling (pCASL) [13] and was performed using a background-suppressed 3D fast spin echo (FSE) technique in the Department of Radiology, Xijing Hospital, at the Fourth Military Medical University. The detailed parameters of 3D-pCASL were as follows: post-labelling delay = 1525 ms; NEX = 3; matrix = 512×512 ; slice thickness = 4.0 mm; TR = 4632.0 ms; bandwidth = 62.5 kHz; and TE = 10.5 ms. In all, the pairs of labelled and control images were obtained. The total acquisition time was 4 min 29 s.

Mice

Idh1^{LSL-R132Q/+} mice were generously donated by Prof. Tak W. Mak of the Ontario Cancer Institute at Princess Margaret Hospital, University Health Network (Toronto, Canada). *Idh1^{LSL-R132Q/+}; Gfap-Cre (Idh1-KI)* mice and the corresponding control *Idh1^{+/+}; Gfap-Cre (Idh1-WT)* mice were generated by breeding *Idh1^{LSL-R132Q/+}* mice [10, 14] with Gfap-Cre transgenic mice (012886, Jax). Animals were maintained under a 12-h on/off light cycle with free access to water and chow diet. Mouse protocols were approved by the Animal Ethics Committee of Fourth Military Medical University.

Cell culture

The parental (HTB14) and IDH1 (R132H) (HTB14IG) U87-MG cells were obtained from ATCC. Cell cultures were maintained in Dulbecco's Modified Eagle's Medium (DMEM; Gibco, USA) containing 10% foetal bovine serum (FBS; ExCell Bio, China) and 100 U/ml penicillin/streptomycin. Cells were cultivated in humidified air in 5% CO₂ at 37 °C at air saturation. To investigate the influences of D-2-HG on the expressions of angiogenesis-related genes, the U87-MG cells were treated with 5 mM or 10 mM D-2-HG (S7873, Selleck) for 24 h, and the protein and mRNA levels were evaluated by immunoblotting and quantitative PCR, respectively.

TCGA gene expression analysis

To analyse the mRNA levels of the PDGFR- β , VEGFA, PDGFB and ANGPT1 in lower-grade gliomas (WHO grade II and III) and GBM, we obtained data from The Cancer Genome Atlas (TCGA) via the cBioportal website (<http://www.cbioportal.org>) [15, 16]. The differences in mRNA levels between IDH-mutated and IDH-wildtype gliomas were analysed by two-tailed Student's *t* tests. The methylation

status of the ANGPT1, PDGFB, VEGFA gene promoters were analysed in 283 cases of lower-grade glioma (TCGA, Provisional), using the Illumina Human Methylation 450 (HM450) assay. A methylated status was defined by a β value greater than 0.20 [17].

Immunohistochemical staining

Hydrated sections were boiled for 15 min in citric acid buffer (pH 6.0), and endogenous peroxidase was inactivated by 3% H₂O₂ in 80% methanol for 20 min. The slides were blocked in relevant serum at room temperature for 1 h and then incubated with the primary antibodies overnight at 4 °C. The primary antibodies included mouse anti-human CD34 (ZM-0046, ZSGB Biotech), mouse anti-human α -SMA (MAB-0006, MXB Biotech), mouse anti-human IDH1(R132H) (MAB-0733, MXB Biotech), rabbit anti-mouse CD31 (77699, Cell Signaling Technology), rabbit anti-human PDGFR- β (C82A3, Cell Signaling Technology) and rabbit anti-rat NG-2 (AB5320, Millipore). After washing with PBS, the slides were incubated with an HRP-labelled secondary antibody for 1 h at room temperature followed by extensive washing. Then, the slides were visualized using diaminobenzidine (DAB), counter-stained with haematoxylin for 1 min, successively dehydrated in increasing concentrations of alcohol gradients, clarified in xylene and then mounted. The immunoreactivity in the specimens was scored according to intensity (0 = negative, 1 = weak, 2 = moderate, 3 = strong staining). The densities of CD34- and α -smooth muscle actin (α -SMA)-positive MVs were counted and analysed in at least five random areas of each glioma slide by experienced pathologists.

Electron microscopy

Mouse brains were removed at birth, fixed in 2.5% cold glutaraldehyde overnight at 4 °C, and then incubated in 1% osmium tetroxide for 1 h at 4 °C. The samples were dehydrated in an ascending ethanol series and embedded in the Epon 812 resin, and ultra-thin sections (70 nm) were cut and placed onto slides. Sections were stained with uranyl acetate and lead citrate and imaged on the JEM-1011 transmission electron microscope.

Quantitative PCR

Total RNA was extracted from the tissues and cultured cells using TRIzol (Invitrogen) according to the manufacturer's instructions. The cDNA was produced by a Primer Script RT Reagent kit (TaKaRa, Japan). Quantitative PCR (qPCR) was performed using the SYBR Green kit (TaKaRa, Japan) on the ABI PRISM 7500 system (Applied Biosystems). The primers used for qPCR are listed in Supplementary Table 1.

Immunoblotting

All proteins were lysed into Radio Immunoprecipitation Assay (RIPA) buffer containing protease inhibitor cocktails (Roche, Switzerland), separated by 10% or 12% SDS-PAGE and transferred onto a PVDF membrane (Millipore). The membranes were blocked with 5% non-fat milk and incubated with appropriate primary antibody at 4 °C overnight, including mouse anti-IDH1(R132H) (MAB-0733, MXB Biotech), mouse anti- β -actin (KM9001, Sungene Biotech), rabbit anti-PDGFR- β (C82A3, Cell Signaling Tech), rabbit anti-PDGFB (ab178409, Abcam), rabbit anti-ANGPT1 (ab183701, Abcam), rabbit anti-VEGFA (190031-1-AP, Proteintech). The membrane was washed with 0.5% Tween-20/PBS three times, and then incubated with appropriate HRP-linked secondary antibodies at room temperature for 1 h. After being extensively washed with PBS, the proteins of interest were detected using enhanced chemiluminescence (ECL) and exposure to X-ray film.

Statistical analysis

All data are expressed as the mean \pm standard error (SE). The results are representative of two or three independent experiments. All statistical analyses were performed using GraphPad Prism software (GraphPad Software, Inc., USA) via paired or unpaired *t*-tests, and differences of $P < 0.05$ were considered statistically significant.

Results

IDH mutation altered the cerebral blood flow of glioma

To evaluate the functions of IDH mutations in the tumour-associated angiogenesis of glioma, the cerebral blood flow (CBF) was assessed by arterial spin labelling (ASL) imaging. As shown in (Fig. 1a), the glioma areas were outlined according T2 Flair, and ASL was acquired using a pseudo-continuous labelling (pCASL) as previously described [13], and performed using a background suppressed 3D fast spin echo (FSE) technique. The relevant areas in other hemispheres were used as controls. The results showed that the mean CBF, max CBF and relative CBF were lower in IDH-mutated astrocytic LGG than those harbouring wildtype IDH (Fig. 1b), which implied that the IDH mutation affected the angiogenesis in glioma.

IDH mutation reduced the pericyte coverage of microvessels in glioma

To determine the effects of IDH mutations on the vasculature, human glioma tissues were analysed by HE and immunohistochemical (IHC) staining with CD34 and

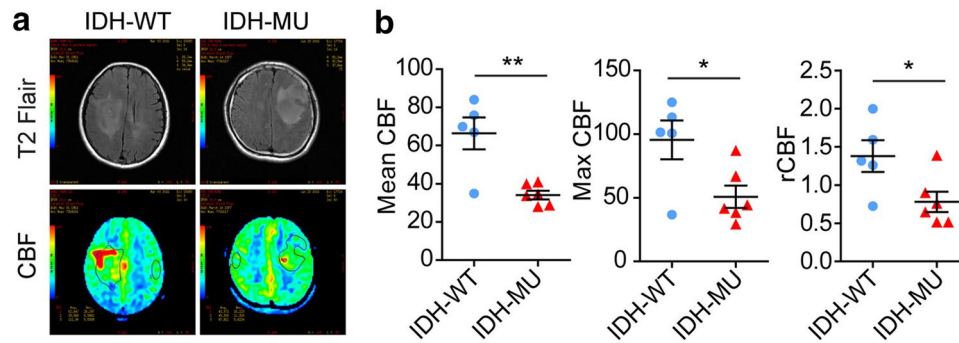


Fig. 1 IDH mutations altered the cerebral blood flow in gliomas. **a** The representative images of cerebral blood flow (CBF) in IDH-wildtype (IDH-WT) and IDH-mutated (IDH-MU) astrocytoma and anaplasia astrocytoma. **b** The statistical results showed that the mean

CBF, max CBF and relative CBF were significantly reduced in IDH-mutated (IDH-MU) gliomas. $n=5$ in IDH-WT group, and $n=6$ in IDH-MU group. * $P < 0.05$ and ** $P < 0.01$

α -SMA. Under HE staining, the walls of MVs in IDH-mutated astrocytic tumour were relatively thinner than those in IDH-wildtype glioma, especially in the LGGs (grades II-III) (Fig. 2a). As a marker of vascular ECs, CD34 outlines all blood vessels in gliomas. The density of CD34 + MVs was increased as the glioma grade increased but was unaffected by IDH mutation (Fig. 2a, b). Furthermore, the staining with α -SMA, a widely used marker of vascular smooth muscle cells (VSMCs), showed that the density of α -SMA + MVs was significantly reduced in IDH-mutated LGG compared to those in the same subtypes with wildtype IDH (Fig. 2a, c). However, the density of α -SMA + MVs was similar in GBMs with different IDH statuses because the proliferative vessels were associated with the formation of complex glomeruloid structures in GBM (Fig. 2a, c). Intriguingly, the statistical analysis indicated that the α -SMA +/CD34 + MV ratio was significantly reduced in IDH-mutated gliomas compared with that in the same subtypes of IDH-wildtype glioma (Fig. 2d). In addition to VSMCs, α -SMA is also detected in pericyte subsets, and these results implied the IDH mutation reduced the pericyte coverages of MVs in glioma.

Moreover, the neural-glial antigen 2 (NG2) and PDGF receptor- β (PDGFR- β), two more specific pericyte markers, were further used to identify the vascular pericytes (Fig. 2e). The immunoblotting and qPCR indicated that the mRNA and protein levels of PDGFR- β were reduced in the IDH-mutated astrocytoma, anaplasia astrocytoma and GBM (Supplementary Fig. 1a, b). In addition, datasets of PDGFR- β mRNA levels were lower in IDH-mutated astrocytic LGG than those harbouring wildtype IDH (Supplementary Fig. 1c). Thus, these results indicated

that pericyte coverage was significantly reduced in IDH-mutated glioma.

Mutant IDH1 knock-in impeded the pericyte coverage of microvessels in mouse brain

A previous study had reported that the brain-specific mutant IDH1 knock-in (KI) mice resulted in haemorrhage. D-2-HG, the product of mutant IDH, could block the prolyl-hydroxylation of collagen, causing a defect in collagen protein maturation [10]. Consistently, our results indicated that the mutant IDH1 knock-in impeded the structures of microvessels in mouse brain (Fig. 3a). The immunohistochemical staining indicated that the densities of α -SMA + MVs were reduced in mutant IDH1 KI brains (Fig. 3b). Under electron microscopy, the pericytes were easily identified in the brains of wildtype mice, but rarely seen in the mutant IDH1 KI brains (Fig. 3c). These results suggested that the mutant IDH1 KI could impede the pericyte coverage of MVs in mouse brain.

IDH mutation reduced the expression of molecules involved in angiogenesis

To explain the mechanisms of how IDH mutation reduced the pericyte coverage in gliomas, the data from The Cancer Genome Atlas (TCGA) were analysed via the cBioportal website (www.cbioportal.org). The results showed that the mRNA levels of the angiogenesis factors, such as *ANGPT1*, *PDGFB* and *VEGFA*, were significantly decreased in IDH-mutated LGG (Grade II and III, $P < 0.001$) compared with IDH-wildtype LGG, and the *ANGPT1* mRNA was also reduced in IDH-mutated GBM (Fig. 4a–c). Furthermore, the

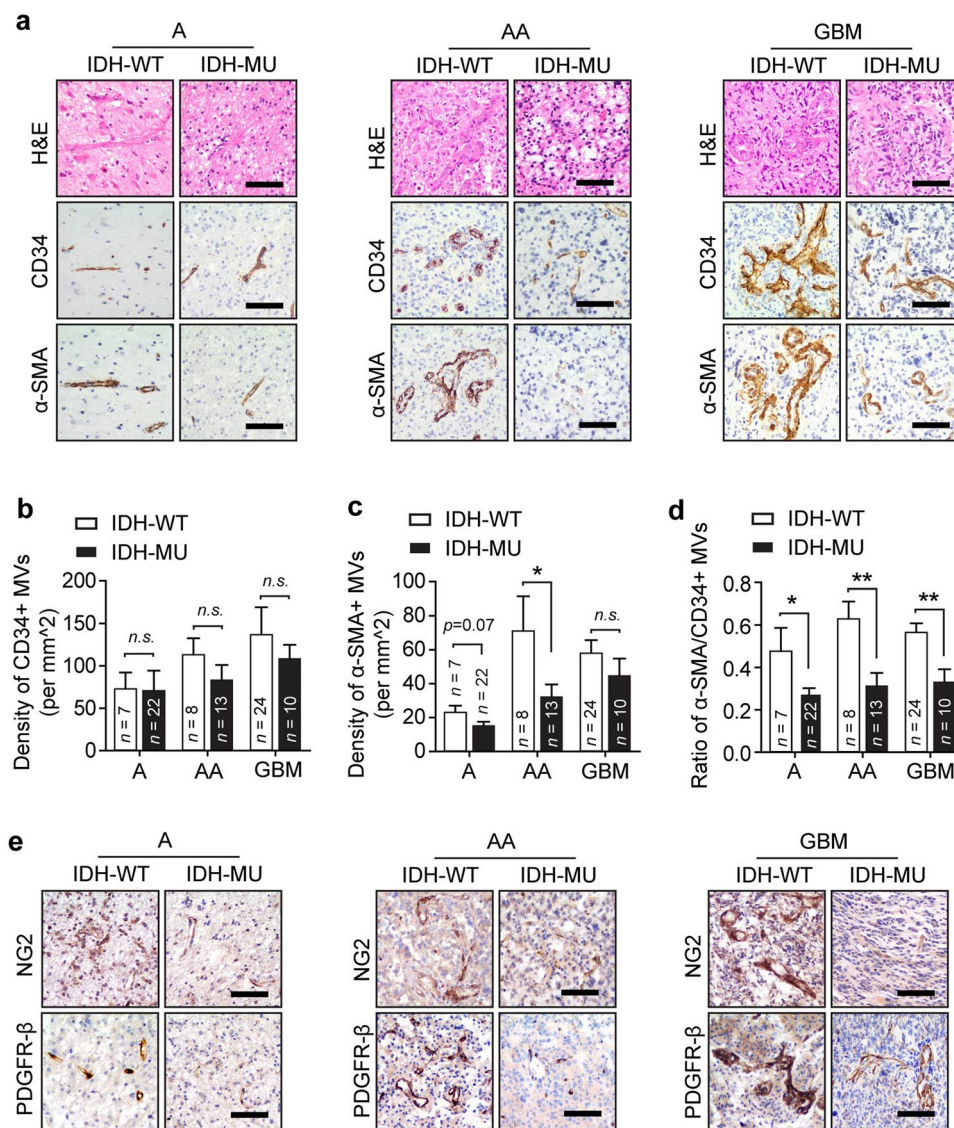


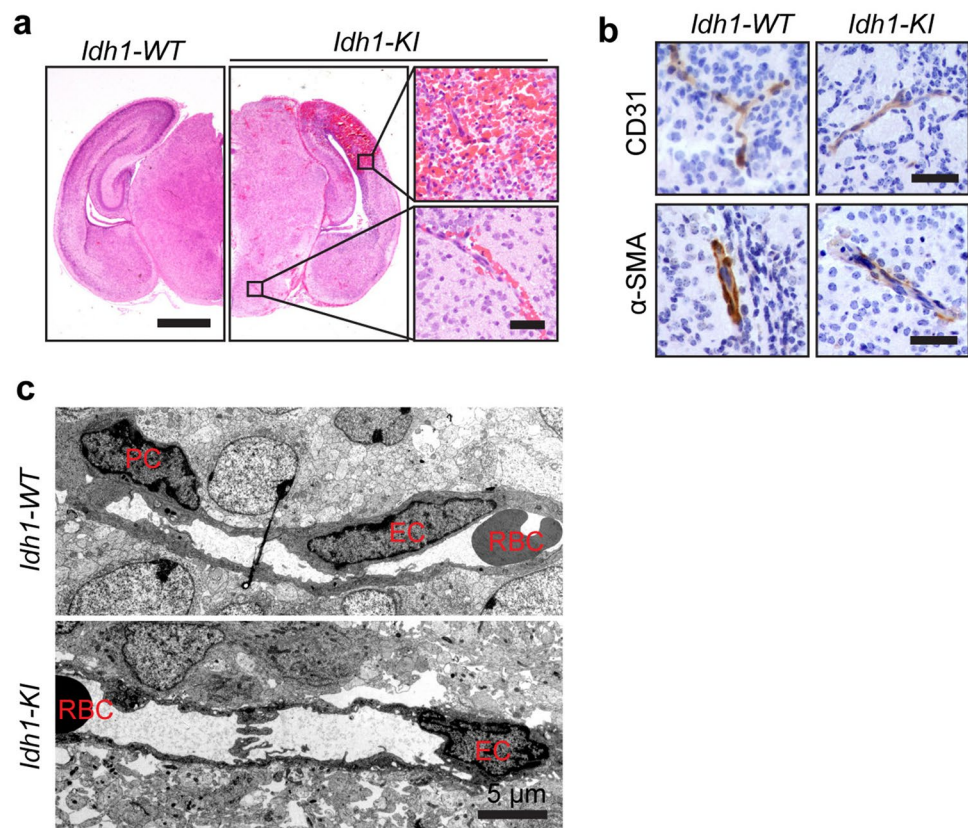
Fig. 2 IDH mutations reduced pericyte coverage in the vasculature of glioma. **a** The MVs in glioma were analysed via HE staining, endothelial cells were immunohistochemically (IHC) stained with CD34, and vascular smooth muscle cells (VSMCs) were labelled with α -SMA. The representative microphotographs of astrocytic tumours, including astrocytoma (A, Grade II), anaplasia astrocytoma (AA, Grade III) and glioblastoma (GBM, Grade IV), showed that the MV densities were similar in the same subtypes of gliomas with different IDH statuses, while the number of α -SMA+MV was significantly reduced in IDH-mutated gliomas (IDH-MU) compared to that in the same subtypes of wild-type IDH gliomas (IDH-WT).

Bar=100 μ m. **b–d** The densities of CD34 and α -SMA+MV were counted and statistically analysed. IDH mutations did not affect the densities of CD34+MV (b) but significantly reduced the density of α -SMA+MV (c) and the ratio of α -SMA/CD34+MV (d) in astrocytoma (A), anaplasia astrocytoma (AA) and glioblastoma (GBM). The data are presented as the mean \pm SE. * P <0.05 and ** P <0.01. **e** The IHC staining of NG2 and PDGFR- β showed that the pericyte coverages of vasculature were significantly reduced in IDH-mutated glioma (IDH-MU) compared to the same subtype with wildtype IDH (IDH-WT). Bar=100 μ m

immunoblotting showed that the protein levels of ANGPT1, PDGFB, and VEGFA were consistently decreased in the IDH1(R132H)-mutated U87-MG cells (Fig. 4d), and the quantitative PCR showed a similar tendency of the mRNA

levels in the IDH-mutated U87-MG cells (Fig. 4e). These results suggested that the IDH mutation reduced the expression of angiogenesis-related genes.

Fig. 3 Mutant IDH1 knock-in impeded the pericyte coverage of vasculature in the brain. **a** *Idh1^{LSL-R132Q/+}* mice were crossed with Gfap-Cre transgenic mice to generate *Idh1^{LSL-R132Q/+}; Gfap-Cre* (*Idh1-KI*) mice and the corresponding control *Idh1^{+/+}; Gfap-Cre* (*Idh1-WT*) animals. The *Idh1-KI* mice suffered from severe cerebral haemorrhage at birth. Bar = 500 μ m (left) or 50 μ m (right). **b** IHC staining showed that the CD31+ endothelium of MVs was relatively normal, but the intensity of α -SMA were reduced in the brains of newborn *Idh1-KI* mice compared to those in the control *Idh1-WT* mice. **c** Electron microscopy (EM) showed that the pericytes were absent around the MVs in the brains of *Idh1-KI* mice. Bar = 5 μ m



D-2-HG inhibited the expression of angiogenesis factors in glioma cells

The mutant IDH obtained a new enzymatic activity to reduce α -ketoglutarate into D-2-HG, which was believed to be an oncometabolite. D-2-HG was proved to competitively inhibit the α -KG-dependent dioxygenases, such as TET1/2, which resulted in the hypermethylation of DNA. The TCGA database showed that the promoters of *ANGPT1*, *VEGFA* and *PDGFB* genes were hypermethylated in the IDH-mutated LGG compared with the IDH-wildtype LGG (Fig. 5a). In vitro, D-2-HG reduced the protein and mRNA levels of *ANGPT1*, *VEGFA* and *PDGFB* in a dose-dependent pattern in U87-MG cells (Fig. 5b, c). These results indicated that D-2-HG inhibited the expression of the angiogenesis factors in glioma, which could explain the reduced pericyte coverage of microvessels in IDH-mutated glioma.

Discussion

Tumour neovascularization is vital for tumour growth and progression, but the nascent microvessels (MV) in tumours are usually characterized by a disordered architecture and abnormal functioning [18, 19]. Abnormal MV architectures

could also reduce the relative cerebral blood volume (rCBV) in tumours, which might lead to hypoxia, insufficient nutrient supply, and resistance to chemo-radiotherapy [19, 20]. In glioma, the rCBV is correlated with the malignancy grade and indicates worse patient outcomes [21], and recent studies have shown that the absolute tumour blood flow, relative tumour blood flow and rCBV were significantly lower in glioma patients with mutant IDH than in those with wildtype IDH [12, 22]. Here, we found that IDH mutation reduced the CBF in glioma, which was consistent with the previous studies [12, 22, 23] and better clinical outcomes of IDH-mutated glioma patients.

Similar to normal microvasculature, tumour vessels consist of two distinct cellular compartments, ECs and pericytes [2], but the pathologic alterations of pericyte coverage in gliomas are poorly understood. In the CNS, pericytes can be found in complex structures composed of microglia cells, neurons, ECs and astrocyte end-feet that together form the so-called functional neurovascular unit (NVU) [24], and the highest pericyte coverage in vasculature has been observed in the CNS [25, 26]. It was widely accepted that the pericytes played essential roles in maintaining the vessel stability and regulating CBF [27–29], although the details of pericytes in controlling CBF are still controversial [30–33]. In the pericyte-deficient mice, the pericyte loss diminished

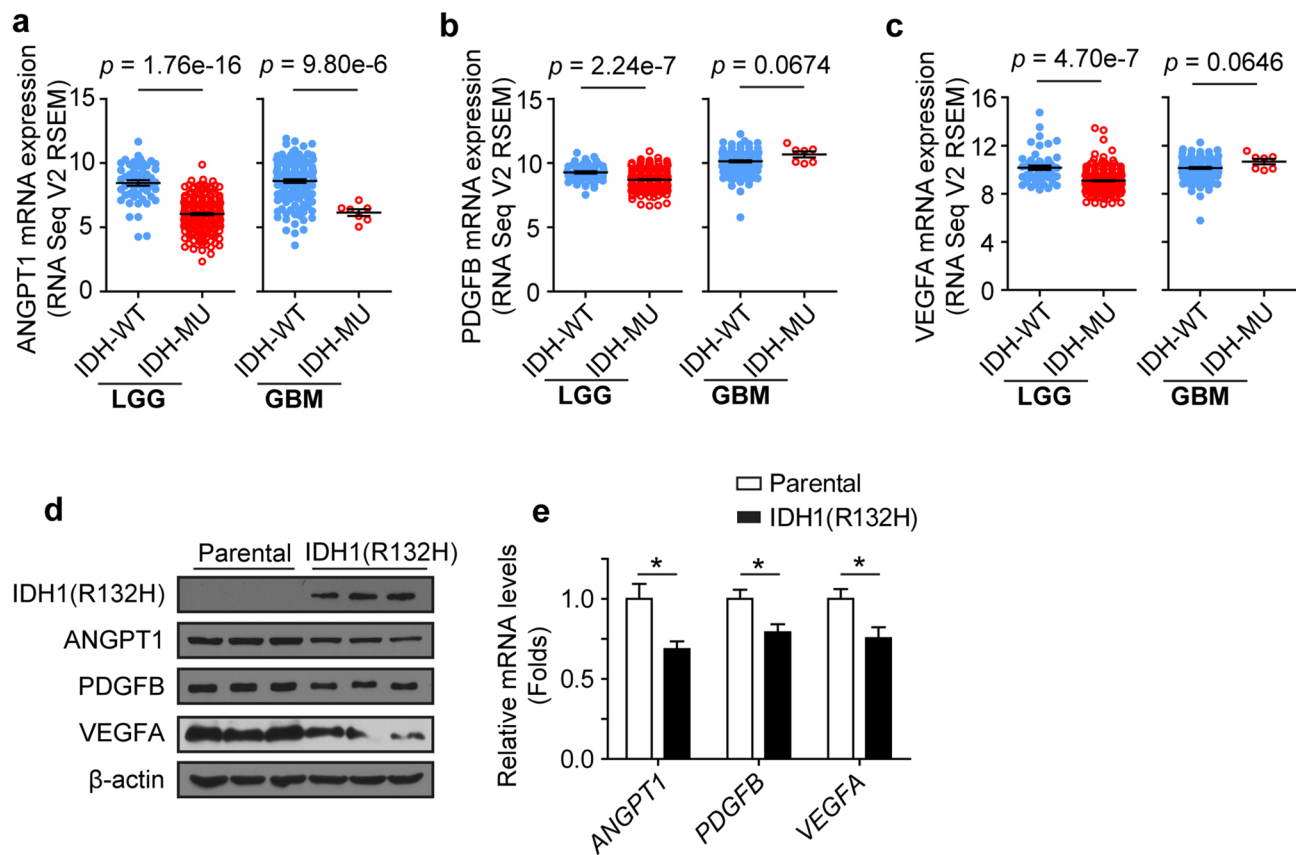


Fig. 4 IDH mutation significantly reduced the expression of angiogenesis factors in glioma. **a–c** The mRNA levels of *ANGPT1* (**a**), *PDGFB* (**b**) and *VEGFA* (**c**) were analysed in lower-grade glioma (LGG) and glioblastoma (GBM) with wildtype IDH (IDH-WT, $n=52$ in LGG and 135 in GBM) and mutant IDH (IDH-MU, $n=131$ in LGG and 7 in GBM) in the TCGA database (<http://www.cbioportal.org/>).

d, e The protein and mRNA levels of ANGPT1, PDGFB and VEGFA in the parental and IDH1(R132H)-mutated U87-MG cells were detected by immunoblotting (**d**) and quantitative PCR (**e**) respectively. The data are presented as the mean \pm SE. $n=3$, * $P < 0.05$ and ** $P < 0.01$

brain capillary perfusion, reduced CBF, and limited oxygen supply to the brain [28, 34]. The pathological characteristics of pericytes could be used as indices of malignant grades in gliomas [5], and the locally proliferated pericytes are the main constituent of MVs in high-grade gliomas. Here, via IHC staining with three specific markers, including α -SMA, NG2 and PDGFR- β , we found that the vascular pericyte coverage was reduced in IDH-mutated gliomas compared with IDH-wildtype glioma. Selectively inhibiting neoplastic pericytes could disrupt the blood-tumour barrier (BTB), thereby increasing drug effusion into established tumours, which highlights the clinical potential of targeting neoplastic pericytes to significantly improve glioma treatment [35].

Mutant IDH lowers the bioavailability of α -KG and increases 2-HG levels, which is believed to competitively inhibit α -KG-dependent dioxygenases, including histone demethylases and the TET family of 5-methylcytosine (5mC) hydroxylases. In IDH-mutant gliomas, DNA

hypermethylation at a large number of loci is thought to be the competitive inhibitor of D-2-HG on DNA demethylases [36]. Several angiogenesis factors, including ANGPT1, PDGF-B and VEGF-A, were involved in pericyte recruitment, migration and proliferation [37], and their expressions were regulated by the promoter of DNA methylation [38–40]. In this study, the results from TCGA databases and IDH1(R132H) mutant U87-MG cells indicated that IDH mutation could reduce the expressions of ANGPT1, PDGFB and VEGFA in gliomas. More importantly, the promoters of *ANGPT1*, *PDGFB* and *VEGFA* genes were hypermethylated in IDH-mutated gliomas. Collectively, our findings suggested that D-2-HG, a product of mutant IDH, might affect the demethylation of the promoter of angiogenesis factors and thus reduced their expressions, which in turn impeded the proliferation of pericytes in gliomas. In all, IDH mutation displayed lower angiogenic gene expression in lower-grade gliomas.

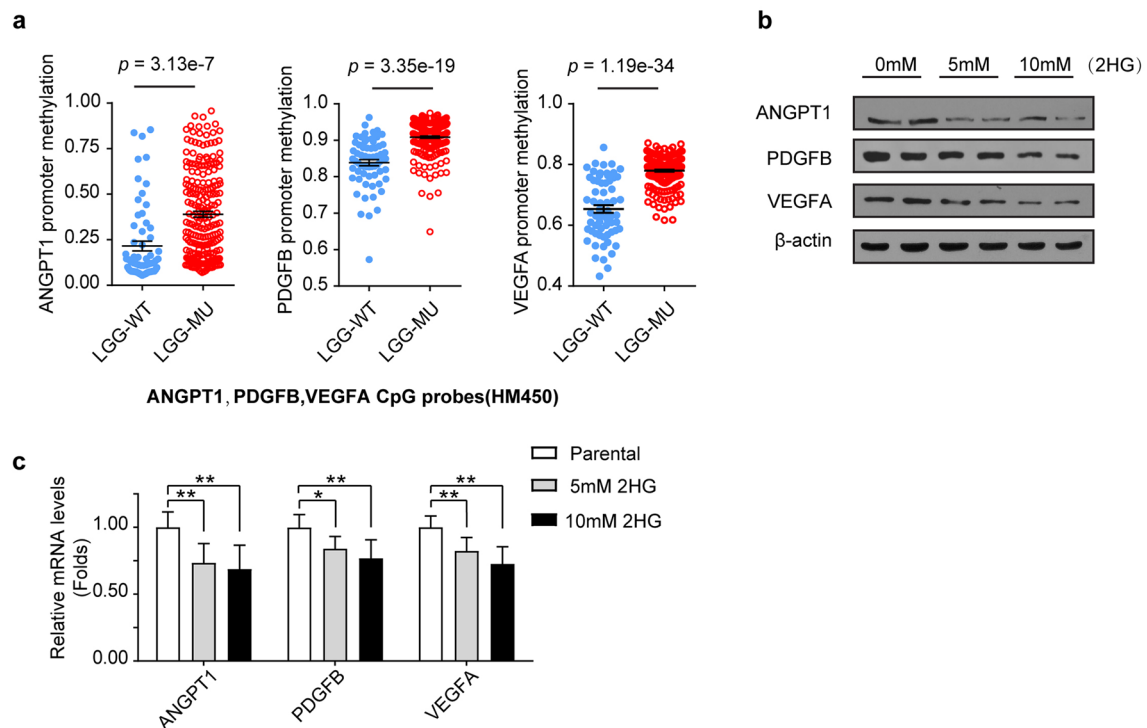


Fig. 5 D-2-HG inhibited the expressions of angiogenesis factors by hypermethylating their promoters. **a** The methylation of *ANGPT1*, *PDGF-B* and *VEGFA* promoters was analysed in the lower-grade glioma (LGG) with wildtype IDH (IDH-WT, n=64) and mutant IDH (IDH-MU, n=218) using CpG probes (HM450) in the TCGA

database (<http://www.cbioportal.org/>). **b, c** The levels of *ANGPT1*, *PDGF-B* and *VEGFA* were detected by immunoblotting (**b**) and qPCR (**c**, n=6) in U87-MG cells treated with 5 mM or 10 mM D-2-HG for 24 h. The data are presented as the mean \pm SE. * $P < 0.05$ and ** $P < 0.01$

In conclusion, IDH mutation downregulated the expressions of angiogenesis factors, which resulted in the lower pericyte coverage of vasculatures in the IDH-mutated glioma. These results are of substantial importance for understanding the functions of IDH mutations in tumour angiogenesis, as well as for the development of novel therapeutic strategies in the IDH-mutated glioma.

Acknowledgements We thank Shengcai Lin for valuable discussion and valuable suggestions.

Funding This study was funded by the National Natural Science Foundation of China (81572471 and 81772659 to J.Y., 81670792 to L.J.Z.; 81372457 to G.C.; 31671416 to P.Z.H.), State Key Laboratory of Cancer Biology (CBSKL2015Z11) and the Booster Program of Xijing Hospital (XJZT15ZL03).

Compliance with ethical standards

Competing interests The authors indicate no potential conflicts of interest.

Ethical approval This article does not contain any studies with human participants performed by any of the authors. Mouse procedure protocols were approved by the Animal Ethics Committee of Fourth Military Medical University.

References


- Jain RK, di Tomaso E, Duda DG, Loeffler JS, Sorensen AG, Batchelor TT (2007) Angiogenesis in brain tumours. *Nat Rev Neurosci* 8:610–622. <https://doi.org/10.1038/nrn2175>
- Bergers G, Song S (2005) The role of pericytes in blood-vessel formation and maintenance. *Neuro-oncology* 7:452–464. <https://doi.org/10.1215/S1152851705000232>
- Winkler EA, Bell RD, Zlokovic BV (2011) Central nervous system pericytes in health and disease. *Nat Neurosci* 14:1398–1405. <https://doi.org/10.1038/nn.2946>
- Cheng L, Huang Z, Zhou W, Wu Q, Donnola S, Liu JK, Fang X, Sloan AE, Mao Y, Lathia JD, Min W, McLendon RE, Rich JN, Bao S (2013) Glioblastoma stem cells generate vascular pericytes to support vessel function and tumor growth. *Cell* 153:139–152. <https://doi.org/10.1016/j.cell.2013.02.021>

5. Sun H, Guo D, Su Y, Yu D, Wang Q, Wang T, Zhou Q, Ran X, Zou Z (2014) Hyperplasia of pericytes is one of the main characteristics of microvascular architecture in malignant glioma. *PLoS ONE* 9:e114246. <https://doi.org/10.1371/journal.pone.0114246>
6. Yan H, Parsons DW, Jin G, McLendon R, Rasheed BA, Yuan W, Kos I, Batinic-Haberle I, Jones S, Riggins GJ, Friedman H, Friedman A, Reardon D, Herndon J, Kinzler KW, Velculescu VE, Vogelstein B, Bigner DD (2009) IDH1 and IDH2 mutations in gliomas. *N Engl J Med* 360:765–773. <https://doi.org/10.1056/NEJMoa0808710>
7. Cohen AL, Holmen SL, Colman H (2013) IDH1 and IDH2 mutations in gliomas. *Curr Neurol Neurosci Rep* 13:345. <https://doi.org/10.1007/s11910-013-0345-4>
8. Ichimura K, Pearson DM, Kocialkowski S, Backlund LM, Chan R, Jones DT, Collins VP (2009) IDH1 mutations are present in the majority of common adult gliomas but rare in primary glioblastomas. *Neuro Oncol* 11:341–347. <https://doi.org/10.1215/15228517-2009-025>
9. Figueroa ME, Abdel-Wahab O, Lu C, Ward PS, Patel J, Shih A, Li Y, Bhagwat N, Vasanthakumar A, Fernandez HF, Tallman MS, Sun Z, Wolniak K, Peeters JK, Liu W, Choe SE, Fantin VR, Paietta E, Lowenberg B, Licht JD, Godley LA, Delwel R, Valk PJ, Thompson CB, Levine RL, Melnick A (2010) Leukemic IDH1 and IDH2 mutations result in a hypermethylation phenotype, disrupt TET2 function, and impair hematopoietic differentiation. *Cancer Cell* 18:553–567. <https://doi.org/10.1016/j.ccr.2010.11.015>
10. Sasaki M, Knobbe CB, Itsumi M, Elia AJ, Harris IS, Chio IL, Cairns RA, McCracken S, Wakeham A, Haight J, Ten AY, Snow B, Ueda T, Inoue S, Yamamoto K, Ko M, Rao A, Yen KE, Su SM, Mak TW (2012) D-2-hydroxyglutarate produced by mutant IDH1 perturbs collagen maturation and basement membrane function. *Genes Dev* 26:2038–2049. <https://doi.org/10.1101/gad.198200.112>
11. Xiong J, Tan WL, Pan JW, Wang Y, Yin B, Zhang J, Geng DY (2016) Detecting isocitrate dehydrogenase gene mutations in oligodendroglial tumors using diffusion tensor imaging metrics and their correlations with proliferation and microvascular density. *J Magn Reson Imaging (JMRI)* 43:45–54. <https://doi.org/10.1002/jmri.24958>
12. Kickingereder P, Sahn F, Radbruch A, Wick W, Heiland S, Deimling A, Bendszus M, Wiestler B (2015) IDH mutation status is associated with a distinct hypoxia/angiogenesis transcriptome signature which is non-invasively predictable with rCBV imaging in human glioma. *Sci Rep* 5:16238. <https://doi.org/10.1038/srep16238>
13. Shen N, Zhao L, Jiang J, Jiang R, Su C, Zhang S, Tang X, Zhu W (2016) Intravoxel incoherent motion diffusion-weighted imaging analysis of diffusion and microperfusion in grading gliomas and comparison with arterial spin labeling for evaluation of tumor perfusion. *J Magn Reson Imaging (JMRI)* 44:620–632. <https://doi.org/10.1002/jmri.25191>
14. Sasaki M, Knobbe CB, Munger JC, Lind EF, Brenner D, Brustle A, Harris IS, Holmes R, Wakeham A, Haight J, You-Ten A, Li WY, Schalm S, Su SM, Virtanen C, Reifenberger G, Ohashi PS, Barber DL, Figueroa ME, Melnick A, Zuniga-Pflucker JC, Mak TW (2012) IDH1(R132H) mutation increases murine haematopoietic progenitors and alters epigenetics. *Nature* 488:656–659. <https://doi.org/10.1038/nature11323>
15. Gao J, Aksoy BA, Dogrusoz U, Dresdner G, Gross B, Sumer SO, Sun Y, Jacobsen A, Sinha R, Larsson E, Cerami E, Sander C, Schultz N (2013) Integrative analysis of complex cancer genomics and clinical profiles using the cBioPortal. *Sci Signal*. <https://doi.org/10.1126/scisignal.2004088>
16. Cerami E, Gao J, Dogrusoz U, Gross BE, Sumer SO, Aksoy BA, Jacobsen A, Byrne CJ, Heuer ML, Larsson E, Antipin Y, Reva B, Goldberg AP, Sander C, Schultz N (2012) The cBio cancer genomics portal: an open platform for exploring multidimensional cancer genomics data. *Cancer Discov* 2:401–404. <https://doi.org/10.1158/2159-8290.CD-12-0095>
17. Agopiantz M, Forgez P, Casse JM, Lacomme S, Charra-Brunaud C, Clerc-Urmes I, Morel O, Bonnet C, Gueant JL, Vignaud JM, Gompel A, Gauchotte G (2017) Expression of neurotensin receptor 1 in endometrial adenocarcinoma is correlated with histological grade and clinical outcome. *Virch Arch* 471:521–530. <https://doi.org/10.1007/s00428-017-2215-y>
18. Bergers G, Benjamin LE (2003) Tumorigenesis and the angiogenic switch. *Nat Rev Cancer* 3:401–410. <https://doi.org/10.1038/nrc1093>
19. Aird WC (2009) Molecular heterogeneity of tumor endothelium. *Cell Tissue Res* 335:271–281. <https://doi.org/10.1007/s00441-008-0672-y>
20. Junttila MR, de Sauvage FJ (2013) Influence of tumour microenvironment heterogeneity on therapeutic response. *Nature* 501:346–354. <https://doi.org/10.1038/nature12626>
21. Law M, Young RJ, Babb JS, Peccerelli N, Chheang S, Gruber ML, Miller DC, Golfinos JG, Zagzag D, Johnson G (2008) Gliomas: predicting time to progression or survival with cerebral blood volume measurements at dynamic susceptibility-weighted contrast-enhanced perfusion MR imaging. *Radiology* 247:490–498. <https://doi.org/10.1148/radiol.2472070898>
22. Yamashita K, Hiwatashi A, Togao O, Kikuchi K, Hatae R, Yoshimoto K, Mizoguchi M, Suzuki SO, Yoshiura T, Honda H (2016) MR imaging-based analysis of glioblastoma multiforme: estimation of IDH1 mutation status. *Am J Neuroradiol (AJNR)* 37:58–65. <https://doi.org/10.3174/ajnr.A4491>
23. Brendle C, Hempel JM, Schittenhelm J, Skardelly M, Tabatabai G, Bender B, Ernemann U, Klose U (2018) Glioma grading and determination of IDH mutation status and ATRX loss by DCE and ASL perfusion. *Clin Neuroradiol* 28:421–428. <https://doi.org/10.1007/s00062-017-0590-z>
24. Sa-Pereira I, Brites D, Brito MA (2012) Neurovascular unit: a focus on pericytes. *Mol Neurobiol* 45:327–347. <https://doi.org/10.1007/s12035-012-8244-2>
25. van Dijk CG, Nieuweboer FE, Pei JY, Xu YJ, Burgisser P, van Mulligen E, el Azzouzi H, Duncker DJ, Verhaar MC, Cheng C (2015) The complex mural cell: pericyte function in health and disease. *Int J Cardiol* 190:75–89. <https://doi.org/10.1016/j.ijcard.2015.03.258>
26. Shepro D, Morel NM (1993) Pericyte physiology. *FASEB J* 7:1031–1038
27. Morikawa S, Baluk P, Kaidoh T, Haskell A, Jain RK, McDonald DM (2002) Abnormalities in pericytes on blood vessels and endothelial sprouts in tumors. *Am J Pathol* 160:985–1000. [https://doi.org/10.1016/S0002-9440\(10\)64920-6](https://doi.org/10.1016/S0002-9440(10)64920-6)
28. Kisler K, Nelson AR, Rege SV, Ramanathan A, Wang Y, Ahuja A, Lasic D, Tsai PS, Zhao Z, Zhou Y, Boas DA, Sakadzic S, Zlokovic BV (2017) Pericyte degeneration leads to neurovascular uncoupling and limits oxygen supply to brain. *Nat Neurosci* 20:406–416. <https://doi.org/10.1038/nn.4489>
29. Svensson A, Ozen I, Genove G, Paul G, Bengzon J (2015) Endogenous brain pericytes are widely activated and contribute to mouse glioma microvasculature. *PLoS ONE* 10:e0123553. <https://doi.org/10.1371/journal.pone.0123553>
30. Attwell D, Mishra A, Hall CN, O'Farrell FM, Dalkara T (2016) What is a pericyte? *J Cereb Blood Flow Metab* 36:451–455. <https://doi.org/10.1177/0271678X15610340>
31. Hill RA, Tong L, Yuan P, Murikinati S, Gupta S, Grutzendler J (2015) Regional blood flow in the normal and ischemic brain is controlled by arteriolar smooth muscle cell contractility and not by capillary pericytes. *Neuron* 87:95–110. <https://doi.org/10.1016/j.neuron.2015.06.001>

32. Winkler EA, Rutledge WC, Kalani MYS, Rolston JD (2017) Pericytes regulate cerebral blood flow and neuronal health at a capillary level. *Neurosurgery* 81:N37–N38. <https://doi.org/10.1093/neuros/nyx457>
33. Hall CN, Reynell C, Gesslein B, Hamilton NB, Mishra A, Sutherland BA, O'Farrell FM, Buchan AM, Lauritzen M, Attwell D (2014) Capillary pericytes regulate cerebral blood flow in health and disease. *Nature* 508:55–60. <https://doi.org/10.1038/nature13165>
34. Bell RD, Winkler EA, Sagare AP, Singh I, LaRue B, Deane R, Zlokovic BV (2010) Pericytes control key neurovascular functions and neuronal phenotype in the adult brain and during brain aging. *Neuron* 68:409–427. <https://doi.org/10.1016/j.neuron.2010.09.043>
35. Zhou W, Chen C, Shi Y, Wu Q, Gimple RC, Fang X, Huang Z, Zhai K, Ke SQ, Ping YF, Feng H, Rich JN, Yu JS, Bao S, Bian XW (2017) Targeting glioma stem cell-derived pericytes disrupts the blood-tumor barrier and improves chemotherapeutic efficacy. *Cell Stem Cell* 21(591–603):e594. <https://doi.org/10.1016/j.stem.2017.10.002>
36. Noushmehr H, Weisenberger DJ, Diefes K, Phillips HS, Pujara K, Berman BP, Pan F, Pelloski CE, Sulman EP, Bhat KP, Verhaak RG, Hoadley KA, Hayes DN, Perou CM, Schmidt HK, Ding L, Wilson RK, Van Den Berg D, Shen H, Bengtsson H, Neuvial P, Cope LM, Buckley J, Herman JG, Baylin SB, Laird PW, Aldape K (2010) Identification of a CpG island methylator phenotype that defines a distinct subgroup of glioma. *Cancer Cell* 17:510–522. <https://doi.org/10.1016/j.ccr.2010.03.017>
37. Armulik A, Genove G, Mae M, Nisancioglu MH, Wallgard E, Niaudet C, He L, Norlin J, Lindblom P, Strittmatter K, Johansson BR, Betsholtz C (2010) Pericytes regulate the blood-brain barrier. *Nature* 468:557–561. <https://doi.org/10.1038/nature09522>
38. Turunen MP, Yla-Herttuala S (2011) Epigenetic regulation of key vascular genes and growth factors. *Cardiovasc Res* 90:441–446. <https://doi.org/10.1093/cvr/cvr109>
39. Culmes M, Eckstein HH, Burgkart R, Nussler AK, Guenther M, Wagner E, Pelisek J (2013) Endothelial differentiation of adipose-derived mesenchymal stem cells is improved by epigenetic modifying drug BIX-01294. *Eur J Cell Biol* 92:70–79. <https://doi.org/10.1016/j.ejcb.2012.11.001>
40. Augello C, Gianelli U, Falcone R, Tabano S, Savi F, Bonaparte E, Ciboddo M, Paganini L, Parafioriti A, Ricca D, Lonati S, Cattaneo D, Fracchiolla NS, Iurlo A, Cortelezzi A, Bosari S, Miozzo M, Sirchia SM (2015) PDGFB hypomethylation is a favourable prognostic biomarker in primary myelofibrosis. *Leuk Res* 39:236–241. <https://doi.org/10.1016/j.leukres.2014.11.012>

Publisher's Note Springer Nature remains neutral with regard to jurisdictional claims in published maps and institutional affiliations.

Affiliations

Chao Sun^{1,2} · Yuanlin Zhao² · Jiankuan Shi^{2,3} · Jin Zhang² · Yuan Yuan² · Yu Gu² · Feng Zhang² · Xing Gao² · Chao Wang⁴ · Yingmei Wang² · Zhe Wang² · Peizhen Hu² · Junhui Qin² · Liming Xiao² · Ting Chang¹ · Liang Wang⁵ · Yibin Xi⁶ · Hong Yin⁶ · Huangtao Chen⁷ · Lijun Zhang⁸ · Guang Cheng⁹ · Jiaji Lin¹ · MingMing Zhang¹⁰ · Zhuyi Li¹ · Jing Ye^{1,2} 

¹ Department of Neurology, Tangdu Hospital, The Fourth Military Medical University, Xi'an 710032, Shaanxi, China

² State Key Laboratory of Cancer Biology and Department of Pathology, Xijing Hospital, The Fourth Military Medical University, Xi'an 710032, China

³ Department of Neurology, Shaanxi People Hospital, Xi'an 710032, China

⁴ Department of Pathology, Chengdu Military General Hospital, Chengdu 610083, China

⁵ Department of Neurosurgery, Tangdu Hospital, The Fourth Military Medical University, Xi'an 710032, Shaanxi, China

⁶ Department of Radiology, Xijing Hospital, The Fourth Military Medical University, Xi'an 710032, Shaanxi, China

⁷ Health Science Center, Xi'an Jiaotong University, Xi'an 710061, Shaanxi, China

⁸ Department of Clinical Laboratory, Tangdu Hospital, The Fourth Military Medical University, Xi'an 710032, China

⁹ Department of Neurosurgery, Xijing Hospital, The Fourth Military Medical University, Xi'an 710032, Shaanxi, China

¹⁰ Department of Cardiology, Tangdu Hospital, The Fourth Military Medical University, Xi'an 710032, Shaanxi, China